Coalescence of nanometer silver islands on oxides grown by filtered cathodic arc deposition

Eungsun Byon, Thomas W.H. Oates[a], and André Anders[b]

Lawrence Berkeley National Laboratory, University of California, 1 Cyclotron Road,

Berkeley, California 94720-8223

August 13, 2002
revised version October 30, 2002

[b] Corresponding Author:

André Anders
Lawrence Berkeley National Laboratory
1 Cyclotron Road
Berkeley, CA 94720-8223
Tel. + (510) 486-6745
Fax + (510) 486-4374
e-mail aanders@lbl.gov

[a] Current address: Applied and Plasma Physics, School of Physics, University of Sydney, 2006, Australia.

1

Coalescence of nanometer silver islands on oxides grown by filtered cathodic arc deposition

Eungsun Byon, Thomas W.H. Oates[a], and André Anders[b]

Lawrence Berkeley National Laboratory, University of California,

1 Cyclotron Road, Berkeley, California 94720-8223

Abstract

Ultrathin silver films have been deposited on glass and oxide-coated glass using filtered cathodic arc deposition and, for comparison, magnetron sputtering. The energetic differences between these deposition methods lead to different film properties. Silver films made by cathodic arc deposition show an earlier onset of island coalescence, indicating that silver islands in energetic deposition exhibit a lower aspect ratio than those produced by evaporation and sputtering. The as-deposited films are thermodynamically unstable, exhibiting changes on a timescale of minutes. While films of islands tend to increase their sheet resistance with time, the sheet resistance of contiguous films shows a decrease. Both effects can be explained by silver mobility driven to minimize film and interfacial energy.

[a] Current address: Applied and Plasma Physics, School of Physics, University of Sydney, 2006, Australia.
[b] Corresponding Author: aanders@lbl.gov (André Anders)

Spectrally selective, transparent coatings are of great interest for energy-efficient window coatings. In cold climates, low-emittance (low-E) coatings with high solar transmittance ($0.3 < \lambda < 3$ μm) and high thermal infrared reflectance ($3 < \lambda < 100$ μm) are required, while in warm climates solar control coatings of high luminous transmittance ($0.4 < \lambda < 0.7$ μm) and high near-infrared reflectance ($0.7 < \lambda < 3$ μm) are beneficial. Both types of coatings can be obtained by embedding a thin metal film between anti-reflecting dielectric layers[1]. It is known that low-emittance and high infrared reflectivity is directly related to the sheet resistance of the metal layer[2]. Silver is currently the metal of choice because of its high conductivity and color-neutral transmission in the visible range of the spectrum. To maximize transmission in the visible and reflectance in the infrared, it is desirable to produce a very thin silver film that is as conducting as possible.

It is known that silver on oxides grows in the Volmer-Weber mode, i.e. silver islands are formed before a continuous film is obtained[3]. Ultrathin silver films that are not continuous (i.e. consisting of islands) show relatively high absorption in the visible and low reflection in the infrared. Coalescence of silver islands is therefore crucial for obtaining the desired optical properties of the coating. Commercially, silver films of about 12 nm thickness are produced for low-E application on a very large scale by magnetron sputtering on oxide-coated flat glass[2]. There are a number of studies on nucleation and growth of metals on oxides, e.g.[1,4-7]. Whilst nucleation, island growth, and coalescence has been investigated for evaporated[8] and sputtered[9] silver films, little is known about silver films synthesized by energetic condensation. In energetic

3

condensation[10,11], film-forming atoms or ions arrive at the substrate surface with hyperthermal energies, typically in the range of 10-100 eV, leading to subplantation and nano-scale thermal spikes around the arriving particle's impact location[12]. Filtered cathodic arc vacuum (FCVA) deposition is a prominent example for energetic condensation. Thin gold films deposited by FCVA deposition have a lower rms. roughness than evaporated and sputtered films[13]. In this work we focus on coalescence of silver on oxide surfaces produced by FCVA deposition. The results will be compared with coalescence of silver islands obtained by magnetron sputtering.

The experimental setup is shown in Fig. 1. A miniature pulsed cathodic arc plasma source[14] with a cylindrical silver cathode of 6.25 mm diameter was operated in the triggerless mode with a ten-stage pulse-forming network.[15] The arc current pulse had a rectangular shape with 1.2 kA amplitude and 620 μs pulse width, with a pulse repetition frequency of 1.6 pulses per second. The plasma source injected streaming silver plasma into a 90° magnetic macroparticle filter[16]. This filter was a curved, open solenoid used to remove microscopic debris ("macroparticles") produced at cathode spots. Neutral silver vapor, if present in the flow, is also removed by the filter, and thus fully ionized silver plasma arrived at the substrates which were located 200 mm from the filter exit. The silver plasma streaming velocity was 11,100 m/s, corresponding to an average kinetic energy of 69 eV, and the mean ion charge state was 2.1 (Ref.[17]). The chamber was cryogenically pumped to a base pressure of about 10^{-4} Pa; no process gas was needed or used.

Uncoated glass standard microscope slides, magnetron-sputtered zinc-oxide-coated glass, and titanium-oxide-coated glass were used as substrates. The samples were mounted on a water-cooled substrate holder. The substrate temperature was generally near room temperature although the surface is subject to heating by the deposition process. It is known[18] that the TiO_2 layer is amorphous while the ZnO layer is polycrystalline with {0001} orientation.

Coalescence of silver islands can be detected by measuring the onset of electronic conduction. The film resistance was measured *in-situ* during deposition. For that purpose, two silver contact pads, approximately 1 μm thick, were deposited on the 25 mm wide samples prior to the experiments. The contact pads were 25 mm apart and thus an area of 25 mm x 25 mm was defined. The resistance between the contact pads was measured using a Keithley 617 micro-ohmmeter, directly giving the sheet resistance in Ohms per square.

The deposition rate was calibrated ex-situ by measuring step heights of a thick film (100 nm) using a Dektak profilometer. The nominal thickness of ultrathin films can easily be determined by counting arc pulses under the assumption that the deposited film thickness is directly proportional to the number of arc pulses. This assumption is generally true but an unknown error may occur at the beginning of the deposition process when the oxide is not yet covered with silver. Unfortunately, this is exactly the regime we are interested in. Therefore, nominal thickness should be understood with this shortcoming in mind. The nominal deposition rate was determined to be 0.023 nm/pulse,

corresponding to about 1/10 of a monolayer per pulse, an instantaneous rate of 37 nm/s and an average rate of 0.037 nm/s.

For comparison, ultrathin silver films have also been deposited in the same process chamber by DC-magnetron sputtering. The same kinds of substrates were placed 100 mm in front of a 3" sputter gun with a silver target. The argon pressure during sputtering was 66 mPa. The sputter power was 40 W with a target potential of –390 V, leading to a deposition rate of 0.75 nm/s.

The essential results are compiled in Fig. 2. The shape of the sheet resistance curves as a function of nominal thickness indicate three regions: (i) the region of individually dispersed clusters and islands, (ii) a transition region where short link conduction starts, and (iii) a region where a continuous film is formed, gradually approaching bulk resistivity when the film thickness much exceeds the electron mean free path (Drude model). The energetics of the deposition process and the substrate material and temperature are known to affect the transition region and formation of a continuous film. This is illustrated by the difference between the curves for cathodic arc and magnetron deposited silver on glass and ZnO.

Focusing initially on filtered arc deposition, it was found that silver on oxides shows a dynamic behavior which is most pronounced in the transition region shown in Fig. 2. At the beginning of the transition, when the sheet resistance was of order 10 MΩ/□, the continuously monitored sheet resistance increased after the cessation of

deposition (Fig 3). To rule out electro-migration induced by the current applied in the measuring process, measurements were several times repeated with the ohmmeter either permanently connected or disconnected between measurements. The sheet resistance changed at the same rate regardless of the ohmmeter being connected or not. As successively more silver was deposited on the substrates, the rate of increase in sheet resistance was observed to slow and eventually reverse (Fig. 3). For films with an initial sheet resistance less than a few 10 kΩ/$\square$, the sheet resistance exponentially decreased over time.

Since this dynamic behavior of a not-yet-continuous silver film occurs on a timescale much longer than the atomic deposition process, it can be anticipated that sputtered films show a similar behavior. The experiments were repeated with DC magnetron sputtering of silver. The results were very similar as shown in Fig. 3.

In the literature, "aging" of thin silver films is discussed. Pattabi *et al.*[19] showed in a ultra-high vacuum system that at low surface coverage, the increase in resistance with time is not due to silver oxidation but due to the mobility of silver leading to the growth of big islands at the expense of smaller islands, minimizing the system's energy. This causes the inter-island spacing to increase and the tunneling current between islands to decrease. Our results at low surface coverage can be interpreted with the same argument.

At greater surface coverage, a contiguous film forms between the contact pads, providing short links and thus electronic conduction other than tunneling. The same driving force as above, minimizing the system's energy, can lead to surface diffusion and the thickening of necks between islands that have coalesced. Electronic transport in films at this growth stage can be described by percolation models.[5,20] With the exception of a very recent publication on sputtered copper films,[7] "aging" towards lower sheet resistance has not been reported.

Due to the different energies involved, nucleation and growth processes for conventional evaporated and sputtered films are thought to be very different from processes by energetic deposition. Nucleation and film growth in conventional deposition occurs *on* the surface of the substrate due to the arrival and motion of film-forming atoms. Nucleation and island formation is governed by adatom mobility,[21] which in turn is determined by the energy of interaction between the surface and the film atoms and the adatom-adatom interaction energy. If the interaction energy between the adatoms and the atoms of the substrate is lower than the energy between the adatoms themselves, the film will grow as discrete islands centered on initial nucleation sites (Volmer-Weber growth). This is known to be the common mode of growth for metal films on insulators.[3,5] Islands grow at the expense of atoms migrating until neighboring islands coalescence, eventually leading to a contiguous and later continuous film.

Nucleation and growth in energetic deposition is different because film-forming ions arrive with high kinetic energy. For example, in the deposition of Ag on TiO_2 using

a filtered cathodic arc, the incident Ag ions have an average kinetic energy of 70 eV, as compared to the 1-3 eV in sputter deposition. Dynamic Monte Carlo simulations[22] using the code T-DYN 4.0 indicate that the kinetic energy causes the silver ions to penetrate the substrate surface with an average range of 1.5 nm, which is several times the mean atomic distance in amorphous TiO_2 (about 0.22 nm). Subplanted silver changes the actual TiO_2 surface, and therefore it is expected that the film-substrate interface energy be different from the interface energy between pure TiO_2 and Ag.

Temperature is a crucial parameter for film growth. "Temperature" in conventional deposition means the substrate temperature, though the situation is more complicated in energetic condensation. Ions deliver both kinetic and potential energy to the substrate[12]. On average, a cathodic arc silver ion delivers 105 eV total energy to the substrate[17], which greatly exceeds the lattice and surface binding energies. While the kinetic energy determines the subplantation range, potential energy contributes to local heating.[12] The total energy is released in a nanoscale thermal spike, when important processes such as diffusion, defect annealing and surface atom migration can occur rapidly. From Molecular Dynamics simulations it is known that thermal spikes are quenched on a picosecond timescale.

The changes that can be observed on a timescale many orders of magnitude longer (Fig. 3) indicate that the quenched configurations are thermodynamically not stable. Even at room temperature, the system is driven by thermodynamic forces that try to minimize the energy stored in the film and its interfaces.[23] For the very thin films

considered here, the energy of the free surface and the interfacial energy with the substrate dominate over strain energy and interfacial energies at grain boundaries.[7] Therefore, the type of substrate material is crucial not only for sputtered films but also for films synthesized by energetic condensation. Regardless of the type of deposition process, our and other[18] experiments show that silver deposition on certain substrates, such as zinc oxide, leads to lower sheet resistance for a given amount of deposited material. The differences can be associated with the island growth and texture development. If the interaction energy between silver and the substrate atoms is high it will reduce the aspect ratio of the islands (defined as the ratio of the maximum height of the island to the island radius), thus reducing the amount of material required to achieve island coalescence. Kinetic energy transfer also facilitates deformation and destruction of existing island structures during energetic deposition, a process known to reduce the island aspect ratio in ion beam assisted film deposition.[24] For thicker films, energy minimization by grain growth will occur. Dannenberg *et al.*[25] found activation energies for 80 nm thick silver films to be 0.53 eV for normal and 0.274 eV for abnormal grain growth, indicating that grain growth is dominated by surface diffusion mass transport. The energy of arriving silver ions exceed these threshold energies by more than 2 orders of magnitude and thus one ion can cause motion of many surface atoms.

In summary, the energetic differences between filtered cathodic arc deposition and magnetron sputtering lead to distinct film properties as shown in Fig. 2. Silver films made by cathodic arc deposition show an earlier onset of island coalescence and formation of short links. This indicates that silver islands in energetic deposition exhibit a

reduced aspect ratio when compared to evaporation and sputtering. The as-deposited films are thermodynamically unstable, exhibiting "aging" on a timescale of minutes. Whilst films of islands tend to increase their sheet resistance with time, contiguous films show a decrease of the sheet resistance. Both effects can be explained by silver mobility driven to minimize the film and interfacial energies. Films made by energetic condensation show lower sheet resistance, implying that low-E and solar control layers made by magnetron sputtering may have still a margin for improvement. Since the world production[2] is of the order of 10^8 m^2 per year, this result can be of economical significance.

References

[1]   G. B. Smith, G. A. Niklasson, J. S. E. M. Svensson, and C. G. Granqvist, J. Appl. Phys. **59,** 571 (1986).

[2]   H. J. Gläser, *Large Area Glass Coating* (Von Ardenne Anlagentechnik GmbH, Dresden, Germany, 2000).

[3]   R. Lazzari and J. Jupille, Surface Sci. **482-485,** 823 (2001).

[4]   S. Xu and B. L. Evans, J. Mat. Sci. **27,** 3108 (1992).

[5]   A. I. Maaroof and B. L. Evans, J. Appl. Phys. **76,** 1047 (1994).

[6]   M. Avrekh, O. R. Monteiro, and I. G. Brown, Appl. Surf. Sci. **158,** 217 (2000).

[7]   E. V. Barnat, D. Nagakura, P.-I. Wang, and T.-M. Lu, J. Appl. Phys. **91,** 1667 (2002).

[8]   B. Gergen, H. Nienhaus, W. H. Weinberg, and E. M. McFarland, J. Vac. Sci. Technol. B **18,** 2401 (2000).

[9]   M. Arbab, Thin Solid Films **381,** 15 (2001).

[10]   O. R. Monteiro, Annual Rev. Mat. Sci. **31,** 111 (2001).

[11]   J. S. Colligon, J. Vac. Sci. Technol. A **13,** 1649 (1995).

[12]   A. Anders, Appl. Phys. Lett. **80,** 1100 (2002).

[13]   A. Bendavid, P. J. Martin, and L. Wieczorek, Thin Solid Films **354,** 169 (1999).

[14]   R. A. MacGill, M. R. Dickinson, A. Anders, O. R. Monteiro, and I. G. Brown, Rev. Sci. Instrum. **69,** 801 (1998).

[15]   A. Anders, R. A. MacGill, and T. A. McVeigh, Rev. Sci. Instrum. **70,** 4532 (1999).

[16]   A. Anders, Surf. Coat. Technol. **120-121,** 319 (1999).

17   A. Anders and G. Y. Yushkov, J. Appl. Phys. **91,** 4824 (2002).

18   R. Dannenberg, D. Glenn, and E. Stach, Proc. 44th Annual Meeting Soc. Vacuum coaters, 218 (2001).

19   M. Pattabi, N. Suresh, S. M. Chaudhari, A. Banerjee, D. M. Phase, A. Gupta, and K. M. Rao, Thin Solid Films **322,** 340 (1998).

20   P. Sheng, Phil. Mag. B **65,** 357 (1992).

21   J. A. Thornton, J. Vac. Sci. Technol. **11,** 666 (1974).

22   J. F. Ziegler, J. P. Biersack, and U. Littmark, *The Stopping and Range of Ions in Solids* (Pergamon Press, New York, 1985).

23   J. M. E. Harper and K. P. Rodbell, J. Vac. Sci. Technol. B **15,** 763 (1997).

24   W. Ensinger, Nucl. Instrum. Meth. Phys. Res. B **127/128,** 796-808 (1997).

25   R. Dannenberg, E. Stach, J. R. Groza, and B. J. Dresser, Thin Solid Films **379,** 133 (2000).

Figure Captions

FIG. 1 Experimental setup for filtered cathodic vacuum (FCVA) arc deposition of thin

metal films.

FIG. 2 Sheet resistance of sputtered and filtered arc deposited silver films as a function of

incident silver dose, which is expressed as nominal film thickness.

FIG. 3 Sheet resistance of silver films on zinc oxide as a function of time after deposition

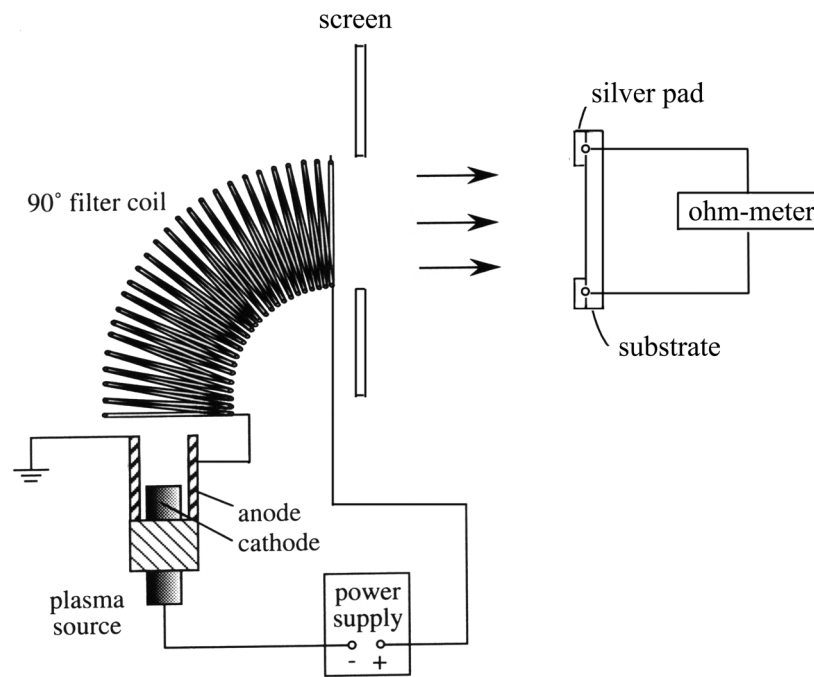was stopped and resistance is continuously monitored.

screen

90° filter coil

silver pad

ohm-meter

substrate

anode
cathode

plasma
source

power
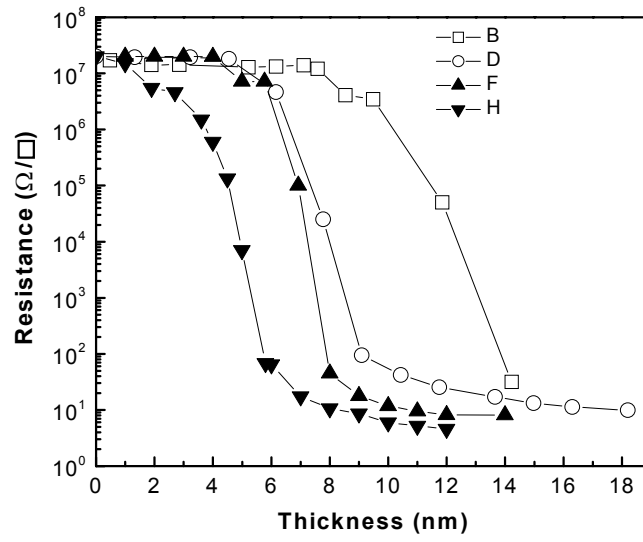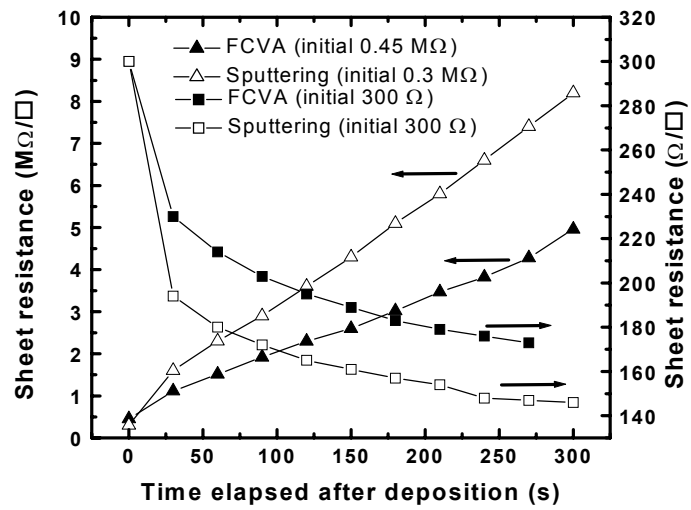supply
- +

Fig. 1, L02-3167

(Byon et. al.)

15

Fig. 2, L02-3167

(Byon et. al.)

Fig. 3, L02-3167

(Byon et. al.)